ELSEVIER

www.elsevier.nl/locate/jorganchem

Journal of Organometallic Chemistry 601 (2000) 211–219

Journal of Organo metallic Chemistry

Optically active transition-metal complexes
Part 124. Chiral 1-phospha[1]ferrocenophanes and 1,12-diphospha[1.1]ferrocenophanes — synthesis, characterization and ring-opening polymerization ☆

Henri Brunner * , Jürgen Klankermayer, Manfred Zabel [1]

Institut für Anorganische Chemie, Universität Regensburg, D-93040 Regensburg, Germany

Received 26 November 1999

Abstract

The phosphorus(III)-bridged [1]ferrocenophanes 1,1′-ferrocenediylphenylphosphine (**1**), (−)-1,1′-ferrocenediylmenthylphosphine (**2**) and (−)-bornyl-1,1′-ferrocenediylphosphine (**3**) have been synthesized via the reaction of 1,1′-dilithioferrocene (TMEDA adduct) and Cl$_2$PR (R = Ph, Men, Bor). Compounds **1** and **2** have been used as ligands in the preparation of the complexes Cp*Mn(CO)$_2$[Fe(η^5-C$_5$H$_4$)$_2$PPh] (**4**) and (−)-*trans*-PdCl$_2$[Fe(η^5-C$_5$H$_4$)$_2$PMen]$_2$ (**5**). The new compounds **2**–**5** were characterized by multinuclear NMR, by MS, and **2**, **4** and **5** by single-crystal X-ray diffraction. Remarkably, the cyclic dimer *anti-exo,exo*-1,12-dimenthyl-1,12-diphospha[1.1]ferrocenophane (**6**) could be isolated and structurally characterized. The thermal ring-opening polymerization of **1**, **2** and **3** yielded the poly(ferrocenediylphosphines) **7**, **8** and **9**. Compounds **2** and **8** were used as chiral ligands in the Rh-catalyzed diastereoselective hydrogenation of folic acid. © 2000 Elsevier Science S.A. All rights reserved.

Keywords: [1]Ferrocenophane; [1.1]Ferrocenophane; Ring-opening polymerization (ROP); Phosphorus; Chirality

1. Introduction

Since their discovery in 1975 [2] [1]ferrocenophanes have attracted attention because of their interesting structures and reactivity [3]. The synthetic potential due to the strained bonding situation in such compounds has been exploited in ring-opening polymerizations (ROPs), which can be conducted under thermal [4,5], anionic [6] or coordination-catalyzed [7] conditions. Although 1-organo-1-phospha[1]ferrocenophanes have been known since 1980 [8], no chiral organic substituent has been used at the phosphorus atom up to now. We prepared 1-phospha[1]ferrocenophanes with chiral substituents at the phosphorus atom and we polymerized them under thermal conditions to obtain polymeric ligands for application in enantioselective catalysis [9].

2. Results and discussion

2.1. Synthesis of (−)-1,1′-ferrocenediylmenthylphosphine (2) and (−)-bornyl-1,1′-ferrocenediylphosphine (3)

Phosphorus-bridged [1]ferrocenophanes, first reported in the 1980s [8,10], were prepared by the reaction of 1,1′-dilithioferrocene (TMEDA adduct) with dichloroorganophosphines Cl$_2$PR (R = Me, ^{t}Bu, Ph) in non-polar solvents such as hexanes. According to the literature [10], 1,1′-ferrocenediylphenylphosphine **1** was synthesized in the reaction of Cl$_2$PPh with 1,1′-dilithioferrocene (TMEDA adduct) in hexanes (Scheme 1). Similarly, the reaction of 1,1′-dilithioferrocene with (−)-dichloromenthylphosphine in hexanes was expected to result in the formation of 1,1′-ferrocenediylmenthylphosphine **2**. Unfortunately, this reaction did not

---

☆ For Part 123, see Ref. [1].

* Corresponding author. Tel.: +49-941-9434441; fax: +49-941-9434439.

E-mail address: henri.brunner@chemie.uni-regensburg.de (H. Brunner)

[1] X-ray structure analyses.

0022-328X/00/$ - see front matter © 2000 Elsevier Science S.A. All rights reserved.
PII: S0022-328X(00)00064-4

work. However, (−)-dichloromenthylphosphine could be converted into the desired [1]ferrocenophane **2** exchanging hexanes by 1,2-dimethoxyethane (DME) (Scheme 1). The preparation of (−)-bornyl-1,1′-ferrocenediylphosphine (**3**) succeeded in hexanes (Scheme 1), but as the diastereomeric purity of the (−)-bornyldichlorophosphine used was 90% de, **3** could only be isolated with a diastereomeric excess of 90%.

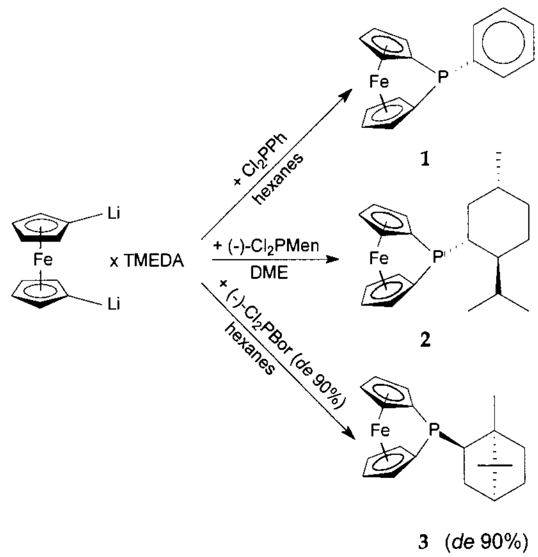

Scheme 1.

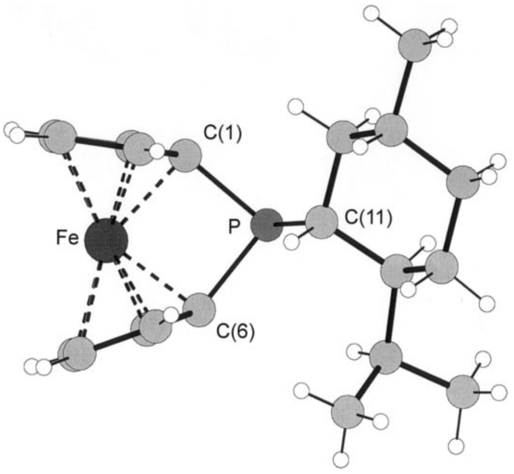

Fig. 1. Molecular structure of **2**.

Table 1
Selected bond lengths (pm) and angles (°) in **2**

Bond lengths			
Fe···P	281.31(7)	P–C(11)	185.8(2)
Fe–C(1)	199.7(2)	Fe–C(6)	199.2(2)
Fe–C(2)	202.2(2)	Fe–C(7)	201.5(2)
Fe–C(3)	208.5(2)	Fe–C(8)	209.0(2)
Fe–C(4)	208.9(2)	Fe–C(9)	209.7(2)
Fe–C(5)	203.2(2)	Fe–C(10)	203.8(2)
Fe···RC1	164.26	Fe···RC2	164.27
Bond angles			
C(1)–P–C(11)	103.48(11)	C(6)–P–C(11)	104.18(10)
C(1)–Fe–C(6)	82.65(9)	C(4)–Fe–C(9)	125.36(9)
C(2)–Fe–C(7)	97.04(10)	C(5)–Fe–C(10)	99.80(12)
C(3)–Fe–C(8)	132.35(11)		

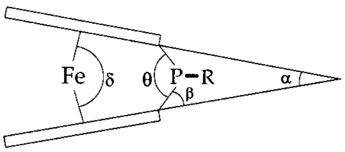

Fig. 2. Assignments of angles in [1]ferrocenophanes.

Compounds **2** and **3** are red solids, which are moderately air sensitive. Both [1]ferrocenophanes are stable under an inert atmosphere in hydrocarbon solvents, but slowly decompose in solvents such as ethanol or THF.

The ^{1}H-NMR spectra of **2** and **3** contain eight resonances for the eight protons of the diastereotopic Cp rings. In the ^{13}C-NMR spectra of **2** and **3** the most striking feature is the high-field shift of the *ipso*-carbon atoms of the [1]ferrocenophane ($\delta_C = 20.1/22.9$ ppm for **2** and $\delta_C = 16.9/22.1$ ppm for **3**). The diastereomeric excess of compound **3** was determined from the intensities of the two ^{31}P-NMR signals at −3.0 and 3.9 ppm.

2.2. X-ray structural analysis of (−)-$Fe(\eta^5\text{-}C_5H_4)_2PMen$ (2)

Dark red crystal of **2** suitable for a single-crystal X-ray diffraction study were obtained from hexanes at −35°C. The distorted sandwich structure of **2** is shown in Fig. 1. Selected bond lengths and angles are given in Table 1. The angles α, β, δ and θ are defined in Fig. 2.

The molecular structure of **2** reveals a tilt angle α between the planes of the Cp rings of 27.43°. This Cp ring tilting in **2** is accompanied by a RC1–Fe–RC2 (RC = ring centroid) angle δ of 159.62°, and a 29.1 pm displacement of the iron atom from the intersection of the two ring centroids. Additional structural distorsions include angles β of 31.27 and 31.58° between the Cp ring planes and the exocyclic C–P bonds. The C(1)–P–C(6) angle θ of 89.80(10)° is quite similar to the angles found in other 1-phospha[1]ferrocenophanes (Table 2) [11,12]. Compared with $Fe(\eta^5\text{-}C_5H_4)_2PPh$ (**1**) [11] and $Fe(\eta^5\text{-}C_5H_4)_2PN^iPr_2$ [12], the Fe···P distance in **2** is slightly longer (281.31(7) vs. 277.4(1) and 280.2(1) pm, Table 2). The distances Fe···RC1 (164.26 pm) and Fe···RC2 (164.27 pm) are very close to the value of 166 pm in ferrocene [13]. Both Cp rings are planar and they are arranged in an ecliptic position.

2.3. Synthesis and X-ray structural analysis of derivatives of **1** and **2**

Compounds **1** and **2** can serve as tertiary phosphine ligands in transition-metal complexes. A dinuclear complex was prepared by treating Cp*Mn(CO)$_2$THF with one equivalent of **1** to give Cp*Mn(CO)$_2$[Fe(η^5-C$_5$H$_4$)$_2$PPh] (**4**) (Scheme 2). The ^{31}P-NMR spectrum of **4** shows the expected downfield shift of the phosphorus resonance from that of the free ligand at $\delta_P = 9.3-109.7$ ppm. In the IR spectrum of **4** two peaks in the carbonyl region at 1922 and 1855 cm^{-1} are detected. For Cp*Mn(CO)$_2$PPh$_3$ the absorptions occur at 1915 and 1855 cm^{-1} [14], confirming the similarity of **1** and PPh$_3$ as ligands.

Table 2
Characteristic bond lengths (pm) and angles (°) [a] in 1-phospha[1]ferrocenophanes, Fe(η^5-C$_5$H$_4$)$_2$PR

	R = ^{t}Bu [11]	R = Ph [11]	R = N^{i}Pr$_2$ [12]	R = Men **2** This study
Fe···P	276.3(1)	277.4(1)	280.2(1)	281.31(7)
Fe–C(1)	198.3(3)	198.2(4)	197.7(2)	199.3(2)
Fe–C(6)	197.8(4)	197.9(4)	198.2(6)	199.2(2)
C(1)···C(6)	263.3(5)	263.2(6)	261.0(2)	263.4(7)
P–C(1)	185.4(3)	184.9(5)	187.4(2)	186.3(2)
P–C(6)	187.0(4)	185.0(5)	185.5(2)	186.9(2)
α	27.1	26.9	27.8	27.43
β (average)	32.8	32.3	41.2(2)	31.4
δ	159.8	159.8	157.1	159.62
θ	90.5(2)	90.7(2)	88.8(1)	89.80(10)

[a] See Fig. 2.

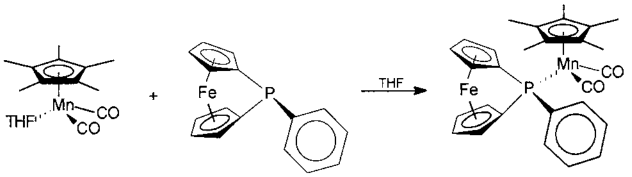

1 **4**

Scheme 2.

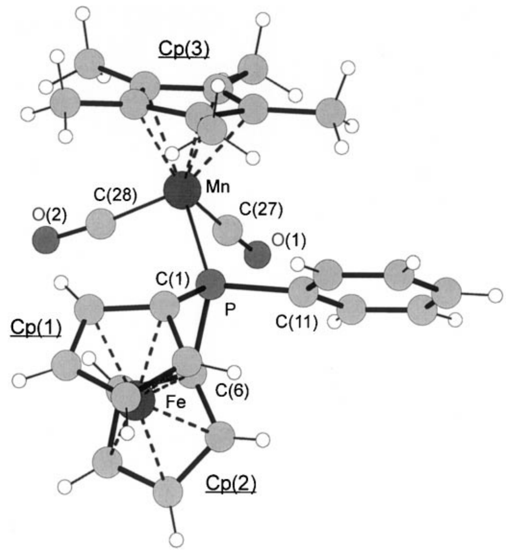

Fig. 3. Molecular structure of **4**.

Table 3
Selected bond lengths (pm) and angles (°) in **4**

P–C(1)	185.85(18)	C(27)–O(1)	116.0(3)
P–C(6)	184.67(19)	C(28)–O(2)	115.9(3)
P–C(11)	182.89(18)	Mn–C(27)	177.1(2)
P···Fe	276.74(5)	Mn–C(28)	177.2(2)
P–Mn	221.13(5)	Fe···RC1	164.16
Fe–C(1)	199.00(19)	Fe···RC2	164.02
Fe–C(6)	199.14(18)	Mn···RC3	177.10
α	26.80(13)	C(1)–P–C(11)	103.59(8)
β	32.66(11)/32.59(12)	C(6)–P–C(11)	102.30(8)
δ	160.25	C(1)–P–Mn	121.91(6)
θ	91.80(8)	C(6)–P–Mn	117.62(6)
P–Mn–C(27)	96.30(6)	C(11)–P–Mn	115.62(6)
P–Mn–C(28)	87.69(6)		
C(27)–Mn–C(28)	92.40(9)		

Orange–brown single crystals of **4** were obtained from hexanes at 5°C. The molecular structure of **4** is shown in Fig. 3. Selected bond lengths and angles are listed in Table 3.

The half-sandwich complex **4** adopts the expected piano stool geometry and the distorted structure of **1** is retained in the complex. Thus, the tilt angle α between the Cp planes (26.80(13) vs. 26.90°) and the Fe···P distance (276.74(5) vs. 277.4(1) pm) are almost the same as for the free ligand **1** [11]. The octahedral geometry of **4** shows up in the angles between the monodentate ligands bonded to the Mn atom, which are around 90° (Table 3).

A trinuclear heterobimetallic complex was prepared by treating Pd(cod)Cl$_2$ with two equivalents of **2** to give (−)-*trans*-PdCl$_2$[Fe(η^5-C$_5$H$_4$)$_2$PMen]$_2$ (**5**) (Scheme 3). In analogy to ligand **2**, complex **5** exhibits an AA′BB′CC′DD′ pattern for the Cp protons in the ^{1}H-NMR spectrum. The ^{31}P-NMR chemical shift of $\delta_P = 49.2$ ppm for **5** is 39.9 ppm downfield compared with **2**, consistent with a coordination of the phosphine **2** to the metal centre.

An X-ray crystal structure determination was carried out for **5**. The molecular structure of **5** is shown in Fig. 4. Selected bond lengths and angles are given in Table 4.

Compound **5** consists of a square-planar *trans*-dichlorodiphosphine-palladium centre, as is usually observed in such complexes [15]. In the C_2 symmetrical complex, the two menthyl groups and the two ferrocenediyl moieties point into the same direction. The tetrahedral geometry of the phosphorus atom is distored by ring strain such that the angle θ between the

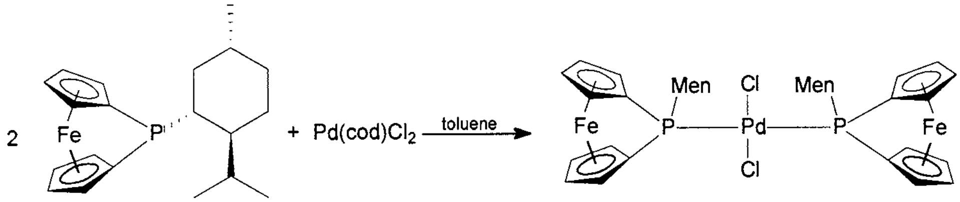

2 **5**

Scheme 3.

two *ipso*-carbon atoms is reduced to 92.43(17)°, compared with 89.80(10)° for the free ligand **2**, whereas the angles between the first menthyl carbon atom and the *ipso*-carbon atoms are 109.89(18) and 106.07(17)°. There is only a slight influence of the coordinating Pd atom on the strained [1]ferrocenophane structure, as the values obtained for α (27.62 vs. 27.43°) and the Fe···P distances (274.15(11) vs. 281.31(7) pm) in **5** and the free ligand **2** are quite similar.

2.4. Synthesis and X-ray structure analysis of *anti-exo,exo-1,12-dimenthyl-1,12-diphospha[1.1]-ferrocenophane* (*6*)

Until we started the present work, the only structurally characterized symmetrical [1.1]ferrocenophanes had bridging atoms from Group 14 (C [16,17], Si [18], Sn [19]) of the Periodic Table. We prepared the first phosphorus-bridged [1.1]ferrocenophane by the reaction of 1,1′-dilithioferrocene with (−)-dichloromenthylphosphine in hexanes at −40°C (Scheme 4). In addition to the dimer **6**, trimers, tetramers and pentamers were found as shown by field desorption mass spectrometry in CH_2Cl_2. The isolation of **6** from the reaction mixture was achieved by medium-pressure liquid chromatography (MLC).

Crystals of the cyclic dimer **6**, suitable for a single-crystal X-ray diffraction study, were obtained from CH_2Cl_2–hexanes at −35°C. Fig. 5 shows the molecular structure of compound **6** and Table 5 lists selected bond lengths and angles.

The molecular structure of **6** consists of two ferrocenediyl units linked in a [1.1]-manner through two PMen bridges and exhibits a chair-like *anti*-conformation. Remarkably, the tilt angles are opposite in direction to those in [1]ferrocenophanes. Thus, for **6** ring tilts of −2.12° (Cp(1) and Cp(3)) and −6.11° (Cp(2) and Cp(4)) were observed. The Cp ligands of the ferrocene parts are staggered by 9.0° (Cp(1) and Cp(3)) and 25.2° (Cp(2) and Cp(4)) (Fig. 6). The phosphorus-bridged Cp rings are twisted by 13.1° (Cp(1) and Cp(2)) and 13.8° (Cp(3) and Cp(4)). Exceptional are the bond angles around the P atoms. Whereas the C(1)–P(1)–C(11) angle is 97.75(18)° and the C(6)–P(1)–C(11) angle is 100.45(17)°, the C(1)–P(1)–C(6) angle is widened to 107.51(19)°. This widening relieves the repulsion of the inner α protons together with the twisting of the ferrocene groups fc-1 and fc-2. The Fe atoms are located symmetrically between the rings with Fe–C distances between 202.7 and 206.7 pm, resulting in a Fe···Fe distance of 504.3(15) pm. This Fe···Fe distance is longer than in the CH_2-bridged [1.1]ferrocenophane (481.6(2) pm), but slightly shorter than in the $SiMe_2$ bridged species (517.1(9) pm) [18,19].

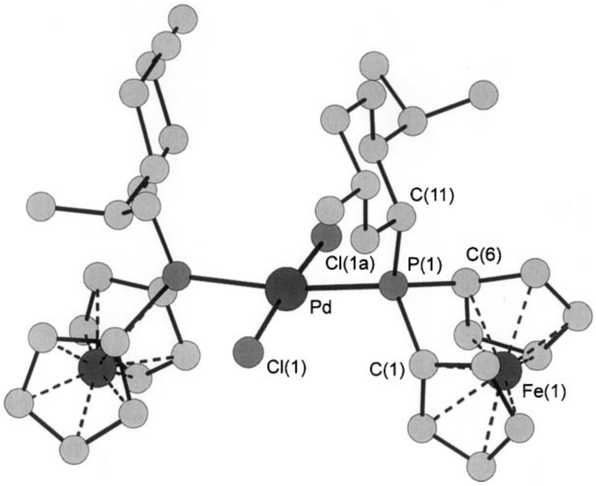

Fig. 4. Molecular structure of **5**. Hydrogen atoms are omitted for clarity.

Table 4
Selected bond lengths (pm) and angles (°) in **5**

Pd–Cl(1)	229.80(7)	Fe(1)–C(1)	198.1(4)
Pd–P(1)	232.53(8)	Fe(1)–C(6)	198.2(0)
P(1)–C(6)	182.5(4)	RC1···RC2	321.64
P(1)–C(1)	181.9(4)	Fe(1)···RC1	163.36
P(1)–C(11)	183.8(5)	Fe(1)···RC2	163.37
Fe(1)···P(1)	274.15(11)		
α	27.6(2)	C(1)–P(1)–C(11)	106.07(17)
β	32.3(5)/32.5(2)	C(6)–P(1)–C(11)	109.89(18)
δ	159.77	C(11)–P(1)–Pd	112.33(12)
θ	92.43(17)	P(1)–Pd–Cl(1)	89.07(3)
Cl(1)–Pd–Cl(1a)	174.32(5)	P(1)–Pd–Cl(1a)	91.38(3)
P(1)–Pd–P(1a)	170.88(5)		

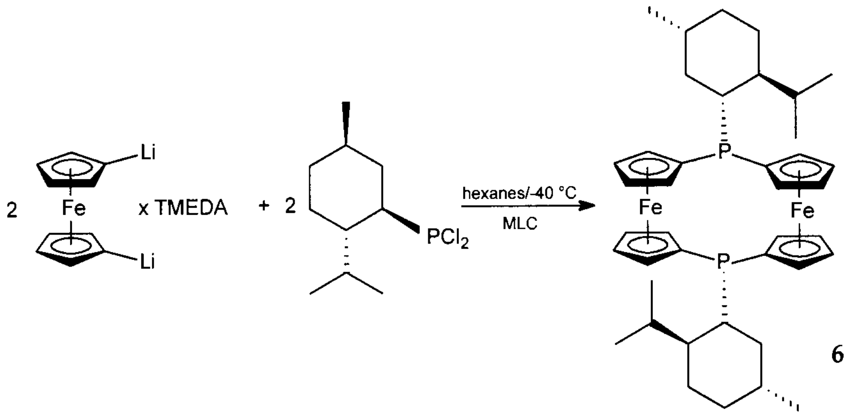

Scheme 4.

2.5. Ring-opening polymerization of **1**, **2** and **3**

Since **2** and **3** have highly strained structures, thermal ROP was expected to result in the formation of the chiral poly(ferrocenediylphosphines) **8** and **9**. Differential scanning calorimetry (DSC) of **2** showed a sharp endothermic peak due to melting at 143°C and a broad exothermic peak at an onset temperature of 191°C due to ring-opening (Fig. 7). For **3** the endothermic melting peak was observed at 102°C and the onset temperature for the polymerization was 183°C (Scheme 5). An estimation of the enthalpy for the ROP process was made on the basis of the integration of the exothermic peak and was found to be ca. 83 kJ mol^{-1} for **2** and 81 kJ mol^{-1} for **3**. By comparison, the enthalpy of polymerization for **1** had been found to be 68 (± 5) kJ mol^{-1} [20] with an onset temperature of 117°C. Consequently, the bulkier chiral groups have a slight effect on the enthalpy, but cause an appreciable increase of the onset temperatures of the polymerization.

An attempt to polymerize **2** and **3** on a preparative scale was carried out by heating the [1]ferrocenophanes at ca. 190–195°C for 2 h. After purification, analysis of the product by NMR was consistent with a ring-opened structure. In particular, the ^{31}P-NMR spectrum of **8** showed only one broad resonance at $\delta_P = -29.3$ ppm with no sign of any residual monomer ($\delta_P = 9.3$ ppm). This upfield shift agrees with the ^{31}P-NMR data reported for **7** in the literature [5]. The ^{1}H-NMR spectrum contained only broad resonances with no signals of the monomer left. In addition, field desorption mass spectrometry of **8** and **9** in CH_2Cl_2 provided evidence for the expected structures showing ions of oligo(ferrocenediylphosphines) of up to eight repeating units.

2.6. Catalytic results

Rhodium complexes, generated in situ from $[Rh(cod)Cl]_2$ and the ligands **2** and **8**, were used as catalysts in the asymmetric hydrogenation of folic acid, in which (−)-BPPM gives 98% hydrogenation and 36.1–42.6% de of the (6*S*,*S*)-isomer of tetrahydrofolic acid [21]. With the [1]ferrocenophane ligand **2** diastereomeric excesses of 20.0 and 22.5% and hydrogenation yields of 28 and 20% were achieved. In contrast, the use of the polymeric ligand **8** gave a high hydrogenation yield (94 and 91%), but only a low diastereomeric excess (2.1 and 2.6%).

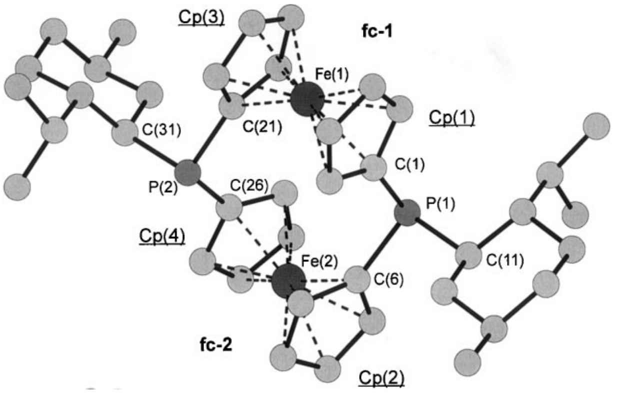

Fig. 5. Molecular structure of **6**. Hydrogen atoms are omitted for clarity.

Table 5
Selected bond lengths (pm) and angles (°) in **6**

Fe(1)···Fe(2)	504.3(15)	P(1)···P(2)	486.6(2)
C(1)–P(1)	182.1(4)	C(21)–P(2)	182.1(4)
C(6)–P(1)	182.1(4)	C(26)–P(2)	183.0(4)
C(11)–P(1)	189.7(4)	C(31)–P(2)	188.2(4)
Fe(1)–RC1	164.31(2)	Fe(2)–RC2	165.53(2)
Fe(1)–RC3	164.70(2)	Fe(2)–RC4	165.89(2)
Fe(1)–C_{Cp} (range)	202.7–205.3	Fe(2)–C_{Cp} (range)	203.3–206.7
C(1)–P(1)–C(11)	97.75(18)	C(21)–P(2)–C(31)	98.09(17)
C(6)–P(1)–C(11)	100.45(17)	C(26)–P(2)–C(31)	98.95(16)
C(1)–P(1)–C(6)	107.51(19)	C(21)–P(2)–C(26)	107.57(18)
RC1–Fe(1)–RC3	179.02	RC2–Fe(2)–RC4	174.91
∠Cp(1)–Cp(3)	2.12	∠Cp(2)–Cp(4)	6.11
∠Cp(1)–Cp(2)	13.84	∠Cp(3)–Cp(4)	13.08

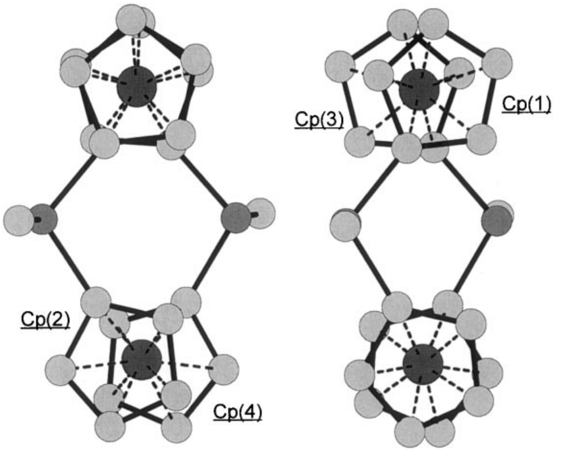

Fig. 6. Top view of **6**. Hydrogen atoms and menthyl groups are omitted for clarity.

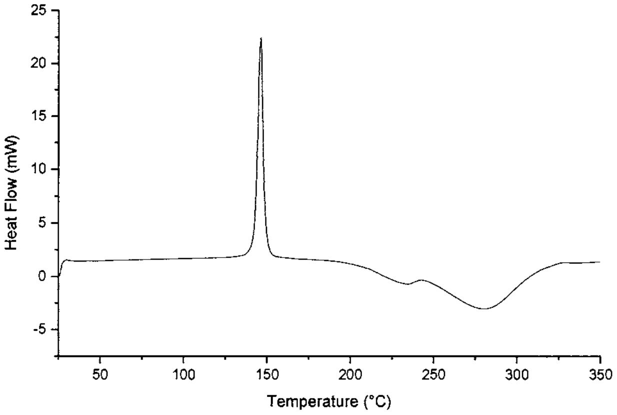

Fig. 7. DSC thermogram of (−)-Fe(η^5-C_5H_4)$_2$PMen (**2**) (10°C min^{-1}).

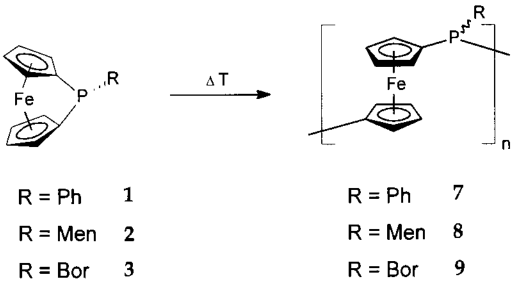

Scheme 5. Thermal ROP of the [1]ferrocenophanes.

3. Experimental

3.1. General considerations

All manipulations and reactions were carried out under an inert atmosphere using standard Schlenk techniques. Reagent-grade solvents were dried and distilled prior to use. Chromatographic materials alumina and silica gel were saturated with N_2. Three acronyms are used successively: Men for the (1*R*,3*R*,4*S*)-menthyl fragment, Bor for the (1*S*,2*R*)-bornyl fragment and fc for the ferrocenediyl fragment.

Melting points: SMP-20 (Büchi), not corrected. Vibrational spectra: Beckman spectrometer IR 4240 (KBr pellets). MS: MAT 311 A (electron impact) and MAT 95 (field desorption), both Finnigan. Optical rotations: Perkin–Elmer 241 polarimeter at room temperature (r.t.). DSC: Mettler–Toledo DSC30 differential scanning calorimeter under nitrogen at a heating rate of 10°C min^{-1}. UV–vis spectra: Kontron Instruments UVIKON 922 spectrophotometer. ^{1}H-NMR spectra: AC 250 (250 MHz, Bruker) and ARX 400 (400 MHz, Bruker). ^{13}C-NMR spectra (including DEPT sequences): ARX 400 (101 MHz). Peak assignments were possible after two-dimensional experiments (COSY). ^{31}P-NMR spectra (^{1}H-decoupled): ARX 400 (162 MHz), external standard 85% H_3PO_4. Elemental analyses: Mikroanalytisches Labor, Universität Regensburg. X-ray structural analyses: STOE IPDS-diffractometer (Mo–K_α radiation, graphite monochromator), SIR97 [22] and SHELXS-97 [23]. A summary of the crystallographic results is presented in Table 6.

Ferrocene, BuLi, (−)-menthol and (−)-borneol were commercial products. The compounds (−)-menthylchloride [24], (−)-bornylchloride [25], (−)-dichloromenthylphosphine [26], (−)-bornyldichlorophosphine [25], 1,1′-dilithioferrocene (TMEDA adduct) [27] and 1,1′-ferrocenediylphenylphosphine **1** [10] were prepared according to literature methods. The asymmetric hydrogenation of folic acid was performed as described [21].

3.2. Preparation of (−)-Fe(η^5-C_5H_4)$_2$PMen (2)

In freshly distilled 1,2-dimethoxyethane (DME) (150 ml), fcLi_2 (TMEDA) (1.57 g, 5.0 mmol) was suspended with stirring at −45°C. To this mixture was added a precooled solution of Cl_2PMen (1.20 g, 5.0 mmol) in DME (30 ml). The resulting mixture was allowed to slowly warm to r.t. Stirring was continued for 2 h. The resulting reaction mixture was filtered, the solvent was removed, and the residue was dried. The resulting solid was dissolved in hexanes and loaded on a basic Al_2O_3 column. A red band eluting with 20:1 hexanes–CH_2Cl_2 was collected. The solution was concentrated and cooled to −35°C, which resulted in the formation of deep red crystals (0.62 g, 1.8 mmol, 35%).

M.p. 131°C. ^{1}H-NMR (C_6D_6): $\delta = 0.79$ (d, $^3J = 6.8$ Hz, 3H), 0.81–0.92 (m, 1H), 0.87 (d, $^3J = 6.3$ Hz, 3H), 0.92 (d, $^3J = 6.7$ Hz, 3H), 0.99 (m, 1H), 1.08 (m, 1H), 1.40 (m, 1H), 1.58 (m, 1H), 1.61–1.66 (m, 1H), 1.65–1.74 (m, 1H), 2.18–2.26 (m, 1H), 2.25 (m, 1H), 2.48 (m, 1H), 4.15 (m, 1H, H_{fc}), 4.19 (m, 1H, H_{fc}), 4.24–4.26 (m, 1H, H_{fc}), 4.28–4.29 (m, 2H, H_{fc}), 4.39–4.41 (m, 1H, H_{fc}), 4.42 (m, 1H, H_{fc}), 4.44 (m, 1H, H_{fc}). ^{13}C-NMR (C_6D_6): $\delta = 16.5$ (s), 20.1 (d, $^1J_{CP} = 48.4$ Hz, *ipso*-C_{fc}), 22.3 (s), 22.9 (s), 22.9 (d, ${}^1J_{CP} = 51.6$ Hz, *ipso*-C_{fc}), 25.6 (d, ${}^3J_{CP} = 11.7$ Hz), 29.4 (d, ${}^3J_{CP} = 9.4$ Hz), 33.8 (d, ${}^3J_{CP} = 9.0$ Hz), 35.1 (d, ${}^2J_{CP} = 11.7$ Hz), 35.2 (s), 37.3 (d, ${}^2J_{CP} = 10.8$ Hz), 49.4 (d, ${}^1J_{CP} = 21.5$ Hz), 76.0–77.8 (m, C_{fc}). ^{31}P-NMR (C_6D_6): $\delta = 9.3$ (s). MS (EI, 70 eV), *m/z* (rel. int.): 354.3 (100) [M]. $[\alpha]_D$ ($c = 0.4$, hexanes) = $-131°$. UV–vis: $\lambda_{max} = 489$ nm, $\varepsilon = 2900$ ($cm^2\ mol^{-1}$). Anal. Calc. for $C_{20}H_{27}FeP$ (354.2): C, 67.80; H, 7.70. Found: C, 67.27; H, 7.72%.

3.3. Preparation of (−)-Fe(η^5-C_5H_4)$_2$PBor (**3**)

In freshly distilled hexanes (100 ml), $fcLi_2$ (TMEDA) (3.02 g, 9.6 mmol) was suspended with stirring and cooled to −78°C. To this mixture was added dropwise by cannula a solution of Cl_2PBor (2.30 g, 9.6 mmol) in hexanes (50 ml). Stirring was continued as the solution was slowly warmed to r.t. over which period (12 h) the color had become dark red. The resulting reaction mixture was then filtered over Celite®, the solvent was removed from the filtrate, and the residue was dried. The resulting solid was dissolved in hexanes and loaded on an Al_2O_3 column. A red band eluting with 20:1 hexanes–CH_2Cl_2 was collected. After removal of the solvent, the residue was dried in vacuo to give **3**. Recrystallization from hexanes afforded deep red needles (1.49 g, 4.2 mmol, 44%).

M.p. 96°C. ^{1}H-NMR (C_6D_6): $\delta = 0.86$ (s, 3H), 0.99 (s, 3H), 1.02 (s, 3H), 1.19–1.34 (m, 2H), 1.45–1.54 (m, 1H), 1.59–1.63 (m, 1H), 1.67–1.77 (m, 1H), 2.06–2.16 (m, 1H), 2.47–2.55 (m, 1H), 2.73–2.79 (m, 1H), 4.18–4.22 (m, 2H, H_{fc}), 4.24–4.29 (m, 3H, H_{fc}), 4.35–4.37 (m, 1H, H_{fc}), 4.41–4.43 (m, 1H, H_{fc}), 4.44–4.46 (m, 1H, H_{fc}). ^{13}C-NMR (C_6D_6): $\delta = 16.6$ (s), 16.9 (d, $J_{CP} = 50.7$ Hz, *ipso*-C_{fc}), 18.8 (s), 19.4 (d, $J_{CP} = 1.8$ Hz), 22.1 (d, $J_{CP} = 55.3$ Hz, *ipso*-C_{fc}), 28.8 (s), 32.2 (d, $J_{CP} = 29.6$ Hz), 34.0 (d, $J_{CP} = 17.7$ Hz), 38.7 (d, $J_{CP} = 9.1$ Hz), 45.5 (d, $J_{CP} = 2.5$ Hz), 48.7 (d, $J_{CP} = 11.3$ Hz), 50.0 (d, $J_{CP} = 3.8$ Hz), 75.8–78.0 (m, 8C, C_{fc}). ^{31}P-NMR (C_6D_6): $\delta = 3.9$ (5%), -3.0 (95%). MS (EI, 70 eV), *m/z* (rel. int.): 352.3 (100) [M]. $[\alpha]_D$ ($c = 0.5$, hexanes) = $-53°$. UV–vis: $\lambda_{max} = 498$ nm, $\varepsilon = 3100$ ($cm^2\ mol^{-1}$). Anal. Calc. for $C_{20}H_{25}FeP$ (352.2): C, 68.19; H, 7.17. Found: C, 68.01; H, 7.22%.

3.4. Preparation of (η^5-C_5Me_5)Mn(CO)$_2$[Fe(η^5-C_5H_4)$_2$PPh] (**4**)

Cp*(CO)$_2$Mn(THF) was prepared from Cp*-(CO)$_3$Mn (310 mg, 1.80 mmol) in THF (200 ml) by irradiation with a medium-pressure Hg arc lamp. 1,1′-Ferrocenediylphenylphosphine **1** (490 mg, 1.70 mmol) in THF (20 ml) was added to the solution at −30°C. The mixture was allowed to warm to r.t. and stirring was continued for 12 h. The solvent was removed. Recrystallization from CH_2Cl_2–hexanes at −35°C gave reddish plates (595 mg, 1.11 mmol, 66%).

M.p. 160°C (dec.). ^{1}H-NMR ($CDCl_3$): $\delta = 1.64$ (s, 15H), 4.27–4.29 (m, 2H, H_{fc}), 4.37–4.42 (m, 2H, H_{fc}), 4.47–4.52 (m, 2H, H_{fc}), 4.92–4.97 (m, 2H, H_{fc}), 7.38–7.85 (m, 5H). ^{13}C-NMR ($CDCl_3$): $\delta = 9.8$ (s), 29.6 (d, ${}^1J_{CP} = 13.6$ Hz), 76.4 (d, $J_{CP} = 4.1$ Hz), 76.5 (d, $J_{CP} = 6.3$ Hz), 77.4 (d, $J_{CP} = 3.5$ Hz), 78.0 (d, $J_{CP} = 8.1$ Hz), 93.0 (s), 128.3 (d, $J_{CP} = 8.8$ Hz), 129.3 (d, $J_{CP} = 1.9$

Table 6
Crystallographic data and experimental parameters for compound **2**, **4**, **5** and **6**

Compound	**2**	**4**	**5**	**6**
Empirical formula	$C_{20}H_{27}FeP$	$C_{28}H_{28}FeMnO_2P$	$C_{40}H_{54}Cl_2Fe_2P_2Pd$	$C_{40}H_{54}Fe_2P_2$
Formula weight (g mol^{-1})	354.24	538.25	885.79	708.47
Crystal system	Monoclinic	Monoclinic	Trigonal	Monoclinic
Space group	$P2_1$	$P2_1/n$	$P3_22_1$	$P2_1$
Z	2	4	3	2
a (Å)	8.3397(8)	8.4816(5)	13.6152(6)	10.0800(7)
b (Å)	10.1177(9)	20.5252(14)	13.6152(6)	12.6670(10)
c (Å)	10.6392(10)	13.7331(14)	18.8645(6)	14.7759(10)
β (°)	104.992(11)	92.643(8)	90	109.563(7)
V (Å^3)	867.16	2388.2(3)	3028.5	1777.7(2)
D_{calc} (Mg m^{-3})	1.357	1.479	1.457	1.324
Absorption coefficient (mm^{-1})	0.956	1.2	1.39	0.933
F(000)	376	1112	1368	752
Theta range (°)	2.53–28.05	1.79–25.66	1.73–25.77	2.1–25.8
Reflections	14876	32678	42585	24734
R_{int}	0.0410	0.077	0.0761	0.057
Data/parameters	4117/307	4502/350	3858/277	6744/525
Goodness-of-fit on F^2	0.997	0.999	0.856	0.913
R_1/wR_2 [$I>2\sigma(I)$]	0.0289/0.0615	0.0339/0.0719	0.0248/0.0413	0.0347/0.0677
R_1/wR_2 (all data)	0.0372/0.0642	0.0422/0.0748	0.0382/0.0434	0.0489/0.0705
Largest difference peak and hole (e Å^{-3})	0.365/−0.291	0.434/−0.299	0.305/−0.211	0.492/−0.254

Hz), 130.4 (d, $J_{CP} = 10.0$ Hz), 138.2 (d, $^1J_{CP} = 37.3$ Hz), 234.7 (d, $^2J_{CP} = 23.8$ Hz, CO). ^{31}P-NMR ($CDCl_3$): $\delta = 109.7$ (s). IR (KBr): 1922, 1855 (C≡O) cm^{-1}. MS (FD, $CHCl_3$), *m*/*z*: 538.1 [M]. Anal. Calc. for $C_{28}H_{28}FeMnO_2P$ (538.3): C, 62.48; H, 5.25. Found: C, 62.19; H, 5.38%.

*3.5. Preparation of (−)-trans-PdCl$_2$[Fe(η^5-C$_5$H$_4$)$_2$PMen]$_2$ (**5**)*

A solution of **2** (150 mg, 0.42 mmol) in toluene (30 ml) was added to a slurry of Pd(cod)Cl_2 (61 mg, 0.21 mmol) in 60 ml of toluene. The mixture was stirred for 12 h and the solvent was removed. Recrystallization from CH_2Cl_2 gave small red crystals (125 mg, 0.14 mmol, 68%).

M.p. 115°C (dec.). ^{1}H-NMR ($CDCl_3$): $\delta = 0.83$ (d, $^3J = 6.6$ Hz, 6H), 0.96 (d, $^3J = 6.5$ Hz, 6H), 1.03 (d, $^3J = 6.6$ Hz, 6H), 1.00–1.12 (m, 2H), 1.19–1.31 (m, 2H), 1.38–1.49 (m, 2H), 1.80–1.89 (m, 2H), 1.90–2.06 (m, 4H), 2.14–2.22 (m, 2H), 2.28–2.39 (m, 2H), 2.48–2.58 (m, 2H), 2.79–2.87 (m, 2H), 4.48–4.50 (m, 2H, H_{fc}), 4.51–4.55 (m, 8H, H_{fc}), 4.63–4.65 (m, 2H, H_{fc}), 4.97–4.99 (m, 2H, H_{fc}), 5.09–5.11 (m, 2H, H_{fc}). ^{31}P-NMR ($CDCl_3$): $\delta = 49.2$ (s). MS (FD, CH_2Cl_2), *m*/*z*: 886.3 (100) [M]. $[\alpha]_D$ ($c = 1.6$, $CHCl_3$) $= -97°$. Anal. Calc. for $C_{40}H_{54}Cl_2Fe_2P_2Pd$ (885.8): C, 54.20; H, 6.15. Found: C, 54.43; H, 6.22%.

*3.6. Preparation of [Fe(η^5-C$_5$H$_4$)$_2$PMen]$_2$ (**6**)*

In freshly distilled hexanes (100 ml), fcLi_2(TMEDA) (0.79 g, 2.5 mmol) was suspended with stirring and cooled to ca. −40°C. To this mixture were added dropwise by cannula 200 ml of a solution of Cl_2PMen (0.60 g, 2.5 mmol) in hexanes. Stirring was continued as the reaction solution slowly warmed to r.t. After 3 h, the slightly reddish mixture was filtered over Celite® and the solvent was removed. The resulting solid was dissolved in CH_2Cl_2 and loaded on an Al_2O_3 column. A yellow band eluting with 1:2 hexanes–CH_2Cl_2 was collected. Purification of the product **6** was achieved with MLC on Merck–Lobar® columns of type B (310 × 25 mm ∅). Recrystallization from 10:1 CH_2Cl_2–hexanes gave small yellow crystals (36 mg, 51 µmol, 2%).

M.p. 170°C (dec.). ^{1}H-NMR (C_6D_6): $\delta = 0.13$–0.24 (m, 2H), 0.41–0.52 (m, 2H), 0.58 (d, $^3J = 6.5$ Hz, 6H), 0.65–0.78 (m, 2H), 0.81 (d, $^3J = 6.9$ Hz, 6H), 0.89 (d, $^3J = 6.9$ Hz, 6H), 0.85–1.01 (m, 2H), 1.04–1.14 (m, 2H), 1.20–1.28 (m, 2H), 1.41–1.53 (m, 2H), 1.60–1.82 (m, 4H), 2.72–2.79 (m, 2H), 4.21–4.23 (m, 2H, H_{fc}), 4.24–4.27 (m, 2H, H_{fc}), 4.32–4.34 (m, 2H, H_{fc}), 4.36–4.38 (m, 2H, H_{fc}), 4.43–4.45 (m, 2H, H_{fc}), 4.45–4.48 (m, 4H, H_{fc}), 4.51–4.54 (m, 2H, H_{fc}). ^{31}P-NMR (C_6D_6): $\delta = -26.7$. MS (FD, CH_2Cl_2), *m*/*z*: 708.2 [M].

*3.7. Thermal ring-opening polymerization of **1**, **2** and **3***

The thermal ROP of **1**, **2** and **3** was carried out as described for the synthesis of polymer **8**.

A small tube was charged with **2** (192 mg, 0.54 mol) and sealed under vacuum (0.01 mmHg). It was heated to 195°C for 2 h. The initially molten sample became immobile after 15 min. After cooling down, the contents were washed with hexanes and dissolved in CH_2Cl_2. The resulting solution was filtered and the solvent was removed to give **8** (125 mg, 0.35 mol, 65%).

Data for polymer **7**: thermal ROP conditions for **1** (from DSC) with 1 h at 120°C; ^{1}H-NMR (CD_2Cl_2): $\delta = 3.6$–4.7 (br, 8H, Cp), 6.8–7.9 (br, 5H, Ph). ^{31}P-NMR (CD_2Cl_2): $\delta = -33.3$ (br).

Data for polymer **8**: thermal ROP conditions (from DSC) for **2** with 2 h at 195°C; ^{31}P-NMR ($CDCl_3$): $\delta = -29.3$ (br). MS (FD, CH_2Cl_2): 708.3 $[M]_2$, 1062.2 $[M]_3$, 1416.2 $[M]_4$, 1770.9 $[M]_5$. Anal. Calc. for $C_{20}H_{27}FeP$ ($[354.2]_n$): C, 67.80; H, 7.70. Found: C, 66.05; H, 7.57%.

Data for polymer **9**: thermal ROP conditions for **3** (from DSC) with 2 h at 190°C; ^{31}P-NMR ($CDCl_3$): $\delta = -34.4$ (br). MS (FD, CH_2Cl_2): 704.2 $[M]_2$, 1056.9 $[M]_3$ to 2818.0 $[M]_8$. Anal. Calc. for $C_{20}H_{25}FeP$ ($[352.2]_n$): C, 68.19; H, 7.17. Found: C, 67.12; H, 6.99%.

4. Supplementary material

Crystallographic data for the X-ray structure analyses have been deposited with the Cambridge Crystallographic Data Centre, CCDC nos. 136996 (**2**), 136993 (**4**), 136995 (**5**), 136994 (**6**). Copies can be obtained free of charge from The Director, CCDC, 12 Union Road, Cambridge, CB2 1EZ, UK (fax: +44-1223-336033; e-mail: deposit@ccdc.ac.uk or www: http//www.ccdc.cam.ac.uk).

References

[1] Part 123: H. Brunner, C. Valério, M. Zabel, New J. Chem., in press.

[2] A.G. Osborne, R.H. Whiteley, J. Organomet. Chem. 101 (1975) C27.

[3] M. Herberhold, Angew. Chem. 107 (1995) 1985; Angew. Chem. Int. Ed. Engl. 34 (1995) 1837.

[4] D.A. Foucher, B.-Z. Tang, I. Manners, J. Am. Chem. Soc. 114 (1992) 6246.

[5] C.H. Honeyman, D.A. Foucher, F.Y. Dahmen, R. Rulkens, A.J. Lough, I. Manners, Organometallics 14 (1995) 5503.

[6] (a) H.P. Withers Jr., D. Seyferth, J.D. Fellmann, P.E. Garrou, S. Martin, Organometallics 1. (1982) 1283. (b) Y. Ni, R. Rulkens, I. Manners, J. Am. Chem. Soc. 118 (1996) 4102. (c) C.H. Honeyman, T.J. Peckham, J.A. Massey, I. Manners, Chem. Commun. (Cambridge) (1996) 2589.

[7] (a) Y. Ni, R. Rulkens, J.K. Pudelski, I. Manners, Makromol. Rapid Commun. 16 (1995) 637. (b) N.P. Reddy, H. Yamashita, M. Tanaka, J. Chem. Soc. Chem. Commun. (1995) 2263.

[8] A.G. Osborne, R.H. Whiteley, R.E. Meads, J. Organomet. Chem. 193 (1980) 345.

[9] J. Klankermayer, Diploma thesis, University of Regensburg, 1999.

[10] D. Seyferth, H.P. Withers Jr., Organometallics 1 (1982) 1275.

[11] I.R. Butler, W.R. Cullen, F.W.B. Einstein, S.J. Rettig, A.J. Willis, Organometallics 2 (1983) 128.

[12] M. Herberhold, F. Hertel, W. Milius, B. Wrackmeyer, J. Organomet. Chem. 582 (1999) 352.

[13] J.D. Dunitz, L.E. Orgel, A. Rich, Acta Crystallogr. 9 (1956) 373.

[14] R.B. King, A. Efraty, W.M. Douglas, J. Organomet. Chem. 56 (1973) 345.

[15] (a) K. Kann, K. Miki, Y. Kai, N. Yasuoka, N. Kasai, Bull. Chem. Soc. Jpn. 51 (1978) 733. (b) K. Miki, Y. Kai, N. Yasuoka, N. Kasai, J. Organomet. Chem. 165 (1979) 79.

[16] A.L. Rheingold, U.T. Mueller-Westerhoff, G.F. Schwiegers, T.J. Haas, Organometallics 11 (1992) 3411.

[17] M. Löwendahl, Ö. Davidsson, P. Ahlberg, M. Håkansson, Organometallics 12 (1993) 2417.

[18] D.L. Zechel, D.A. Foucher, J.K. Pudelski, G.P.A. Yap, A.L. Rheingold, I. Manners, J. Chem. Soc. Dalton Trans. (1995) 1893.

[19] F. Jäkle, R. Rulkens, G. Zech, D.A. Foucher, A.J. Lough, I. Manners, Chem. Eur. J. 4 (1998) 2117.

[20] T.J. Peckham, A.J. Lough, I. Manners, Organometallics 18 (1999) 1030.

[21] H. Brunner, P. Bublak, M. Helget, Chem. Ber./Recl. 130 (1997) 55.

[22] A. Altomare, G. Cascarano, C. Giacovazzo, A. Guagliardi, J. Appl. Crystallogr. 26 (1993) 343.

[23] G.M. Sheldrick, SHELXL97, Program for Crystal Structure Refinement, University of Göttingen, Germany, 1997.

[24] J.G. Smith, G.F. Wright, J. Org. Chem. 17 (1952) 1116.

[25] A. Marinetti, F.-X. Buzin, L. Ricard, J. Org. Chem. 62 (1997) 297.

[26] H. Brandes, R. Goddard, P.W. Jolly, C. Krüger, R. Mynott, G. Wilke, Z. Naturforsch. Teil B 39 (1984) 1139.

[27] (a) R.F. Kovar, M.D. Rausch, H. Rosenberg, Organomet. Chem. Synth. 1 (1970/1971) 173. (b) J.J. Bishop, A. Davidson, M.L. Katcher, D.W. Lichtenberg, R.E. Merill, J.C. Smart, J. Organomet. Chem. 27 (1971) 241.